

# Effect of TEA on characteristics of CdS/PbS thin film solar cells prepared by CBD

H. SATTARIAN<sup>1</sup>, T. TOHIDI<sup>2\*</sup>, SH. RAHMATALLAHPUR<sup>2</sup>

<sup>1</sup>Department of Physics, Maragheh Branch, Islamic Azad University, Maragheh, Iran

<sup>2</sup>Northwest Research Complex, NSTRI, Bonab, Iran

In this study, a solar cell with a glass/ITO/CdS/PbS/Al structure was constructed. Both window (CdS) and absorption (PbS) layers were deposited by chemical bath deposition (CBD) method. The CdS window layer was deposited on ITO-glass. The PbS nanocrystalline thin film was prepared with and without triethanolamine on CdS films at bath temperature of 25 °C. CdS and PbS nanocrystals were identified using XRD and SEM. The cells are photosensitive in a large spectral range (at visible and near infrared regions). The cell with absorbing layer obtained from the bath without TEA has higher efficiency with the following parameters: the open circuit voltage ( $V_{oc}$ ) is 275 mV, short circuit current ( $J_{sc}$ ) is 12.24 mA/cm<sup>2</sup>, maximum voltage ( $V_{max}$ ) is 165 mV and maximum current ( $J_{max}$ ) is 7.11 mA/cm<sup>2</sup> with the efficiency  $\eta = 1.31\%$ , fill factor FF is 32% under the illumination intensity of 90 mW/cm<sup>2</sup>. The cells have an area of 0.15 cm<sup>2</sup>.

Keywords: *nanocrystalline films; solar cell; chemical bath deposition*

© Wrocław University of Technology.

## 1. Introduction

In the development of photovoltaic solar cell devices, one of the most important issues is the cost of production process, including the cost of materials and the cost of technological processes. Yet another aspect is the ecological one: the devices for production of clean energy need clean technology. Among various technologies available nowadays, photovoltaics (PV) is believed to be one of the cleanest ways in achieving this goal. However, efforts are still needed to make photovoltaic cost competitive over other established technologies for energy production.

Integration of nanostructured materials in photovoltaic devices has been demonstrated to open the possibilities to develop low-cost solar cells. Because of their fundamental structural, electrical and optical properties resulting from quantum confinement, nanocrystalline inorganic materials have been widely studied for solar cell application [1]. PbS is a unique semiconductor material with a small band gap (0.41 eV at 300 K) and large

bulk exciton Bohr radius (18 nm). This band gap can be easily manipulated by altering the semiconductor dimensions and can reach a few eV for PbS particles in the nanometer range [2]. This property of PbS makes it desirable for new applications such as solar cells [3]. PbS is an absorbent material that can be coupled with CdS layers in solar cells. Cadmium sulfide (CdS) is an important II – VI semiconductor having a wide band-gap of 2.4 eV with well-known applications in lasers, light-emitting diodes, solar cells, etc. [4]. CdS is used as a buffer material for high efficiency polycrystalline thin film solar cells [5].

Both physical and chemical methods for the deposition of macro- and nanocrystalline PbS and CdS have been described in literature. Among the chemical methods, chemical bath deposition (CBD) is of special interest because it is simple and highly efficient. CBD allows adjustable control of size and surface density of nanoparticles, and can be used for preparation of high-quality nanocrystalline PbS and CdS films [4, 6]. This method has been shown to allow control of stirring period, reaction time, bath temperature, pH of solution, complexing agent and impurities [7, 8].

\*E-mail: m.tohidi@azaruniv.edu

Among several n-type semiconductor materials, it has been observed that CdS is the most promising heterojunction partner for the well-known polycrystalline photovoltaic material as a window layer [5]. CdS films have been the most widely used as the most successful n-type window layer for high efficiency thin film solar cells based on CdTe [9] and Cu (InGa)Se<sub>2</sub> (CIGS) [10]. Nair et al. [11] have prepared CdS as a window layer for CdS/PbSe solar cell. Recently, Bhandari et al. [12] have reported on heterojunction colloidal PbS quantum dot (QD) solar cells using RF magnetron sputtered CdS as the n-type window layer. Hernandez-Borja et al. [13] have fabricated CdS/PbS solar cell with CdS window layer. They deposited CdS window layers via ammonia-free CBD process. Obaid et al. [14] have reported on n-CdS/p-PbS heterojunction solar cells obtained by microwave-assisted chemical bath deposition (MACBD) method.

The fabrication of high efficiency and low cost solar cells is always of great importance and remains a hot topic for scientists. The present study, in addition to the basic materials, uses triethanolamine (TEA) as a complexing agent in the chemical bath for the preparation of PbS and CdS films. A metal complex  $[Pb(TEA)]^{2+}$  forms when TEA is added to the bath. The TEA acts as a complexing agent to prevent direct precipitation of PbS and controls the interaction of  $Pb^{2+}$  and  $S^{2-}$  ions during film formation. PbS films were also prepared without TEA by the CBD method to obtain thicker PbS films. Structure and microstructure as well as optical properties of both PbS and CdS thin films prepared using the CBD method, were investigated. The prepared PbS films with and without TEA were investigated on the fabricated PbS/CdS solar cells.

## 2. Experimental

### 2.1. Preparation of CdS and PbS thin films

All chemicals were of analytical grade (Merck) and we used them as received without further purification. The total device structure was

as follows: glass/ITO/CdS/PbS/Al (Fig. 1). For making the device, first the conducting glass/ITO commercial substrates with a sheet resistance of  $25 \Omega/\square$  were washed with soap in hot distilled water and rinsed many times in distilled water. Then, the substrates were cleaned ultrasonically by distilled water for 30 min and dried under nitrogen atmosphere.

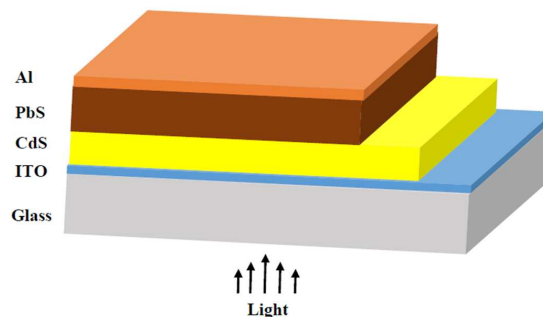
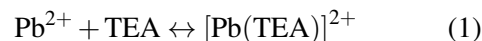


Fig. 1. Schematic diagram of a fabricated solar cell.

CdS thin films were prepared from a chemical bath containing 0.2 M CdCl<sub>2</sub>, 1 M thiourea, 1 M triethanolamine (TEA) and 2 M ammonium hydroxide (NH<sub>4</sub>OH). The temperature and pH value of the bath were 75 °C and 10 pH, respectively. In general, the prepared films were homogeneous, smooth, and adherent to the substrate.

PbS thin films were deposited on glass (for optical studies) and on glass/ITO/CdS structure by CBD at room temperature. The bath contained an aqueous solution of 0.5 M lead acetate, 1 M thiourea, 2 M sodium hydroxide and 1 M triethanolamine. The pH value was adjusted to 12 in all baths. Although at the beginning the bath was colorless, its color changed to brown and then to black. The probable reaction for PbS thin film formation were reported in our previous work [15].

With the addition of TEA as the complexing agent, the metal complex is formed [15]:



The complexing agent helps to control the reaction rate. The formation of the metal complex reduces the concentration of free  $Pb^{2+}$  ions below the level required for the precipitation of solid

phase  $\text{Pb}(\text{OH})_2$ . The formation of nucleation centers through  $\text{Pb}(\text{OH})_2$  in the reaction bath is the first step in the growth of PbS film on the substrates.

After deposition, the samples were rinsed in deionized water. The non-adherent outer PbS layer was then removed with a cotton swab dipped in a dilute ammonium sulphate solution and again rinsed.

A 160 nm thick aluminum (Al) film was used as the bottom contact. It was deposited either by electron beam evaporation or thermal evaporation methods.

## 2.2. Analysis instrumentation

The structure of the films was analyzed by X-ray diffraction (XRD) using D8-advanced Bruker and  $\text{CuK}\alpha$  radiation ( $\lambda = 1.5406 \text{ \AA}$ ) equipment. A UV-Vis double-beam spectrophotometer (T80 UV-Vis, PG Instruments) was used to record the absorption spectra. The surface morphology of the deposited films was characterized using SEM (XL 30-Philips).

## 3. Results and discussion

### 3.1. XRD studies

XRD spectra of the as-deposited CdS thin films shown in Fig. 2a have been used for evaluation of the crystallographic properties of the CdS thin films. The diffraction spectra were obtained by scanning in the  $2\theta$  range of  $20^\circ$  to  $80^\circ$ . The most attractive feature of CdS thin films prepared by CBD, from structural point of view, is its polymorphism. As a matter of fact, cubic and hexagonal crystalline structures in CdS films were generally reported by many authors. As seen, the obtained diffraction pattern shows a predominant peak at  $2\theta = 26.6^\circ$  which can be assigned to the (1 1 1) plane of cubic CdS [17, 18]. As shown in Fig. 2a, the film shows also two diffraction peaks at  $44.3^\circ$  and  $52.3^\circ$  which are assigned to the (2 2 0) and (3 1 1) reflection planes in the CdS cubic structure. The broadening of the diffraction peaks indicates the nanocrystalline nature of the samples.

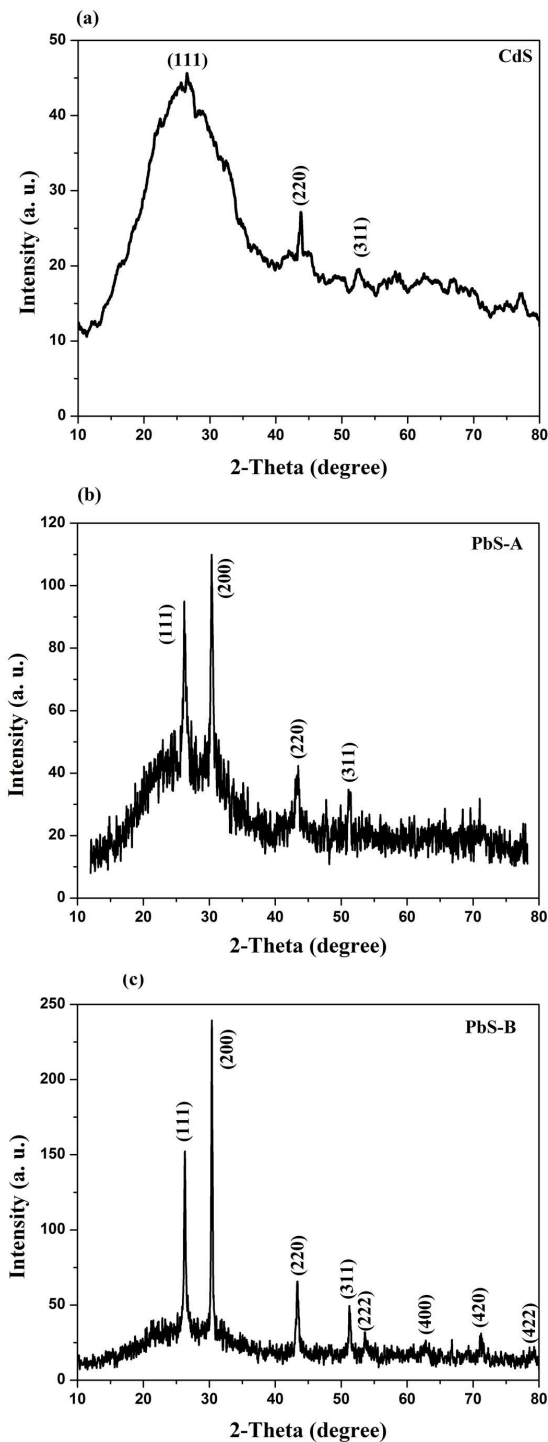


Fig. 2. XRD patterns of (a) CdS thin films and PbS films (b) with and (c) without TEA.

Fig. 2b and Fig. 2c show the X-ray diffraction patterns of PbS films obtained from the bath

with (PbS-A) and without (PbS-B) TEA. The PbS-A films have produced only peaks at  $26.221^\circ$ ,  $30.361^\circ$ ,  $43.481^\circ$ , and  $51.241^\circ$ , corresponding to the Miller planes (1 1 1), (2 0 0), (2 2 0), and (3 1 1), respectively (Fig. 2b). However, the patterns in Fig. 2c clearly show diffraction peaks at  $26.411^\circ$ ,  $30.501^\circ$ ,  $43.501^\circ$ ,  $51.471^\circ$ ,  $53.861^\circ$ ,  $69.331^\circ$ ,  $71.361^\circ$ , and  $79.361^\circ$ , which correspond to the (1 1 1), (2 0 0), (2 2 0), (3 1 1), (2 2 2), (3 3 1), (4 2 0), and (4 2 2) planes of the PbS phase with cubic structure. The intensity of the peaks in PbS-B films is higher than those of the PbS-A films, because the thickness of the PbS-B films is larger than that of the PbS-A films.

The influence of crystallite size on the electrical and optical behavior of the films is very important. The average crystallite size of CdS was calculated to be 11 nm using the Debye-Scherrer formula,  $D = K\lambda/\beta_{2\theta}\cos\theta$ , where  $D$  is the crystallite size,  $\lambda$  is the wavelength of the X-ray radiation ( $1.5406 \text{ \AA}$ ),  $K$  is usually taken as 0.9,  $\theta$  is the Bragg angle, and  $\beta_{2\theta}$  is the line width at half-maximum height. The average crystallite sizes obtained for PbS-A and PbS-B sample were 25 nm and 250 nm, respectively. The crystallite size for PbS-B was greater than those for PbS-A. When TEA was added to the chemical bath, fewer ions were available for the film formation, so thinner films were formed, resulting in the formation of small grain sizes. To grow a film on a substrate using CBD, the first step is the formation of nucleation centers through the  $\text{Pb(OH)}_2$  in the reaction bath and the second step is the growth stage. Nucleation is generally attributed to the formation of tiny seeds with well-defined crystallinity and a stable structure. In thinner films the number of tiny seeds for growing is low so the grain size is small.

### 3.2. SEM studies

Fig. 3 shows scanning electron microscopy (SEM) images of the deposited films. Fig. 3a indicates that CdS thin film is covered completely; no pinholes or cracks can be observed. Fig. 3b and Fig. 3c shows the SEM images of the PbS-A and PbS-B thin films, respectively. It can be seen from the SEM images that both groups form

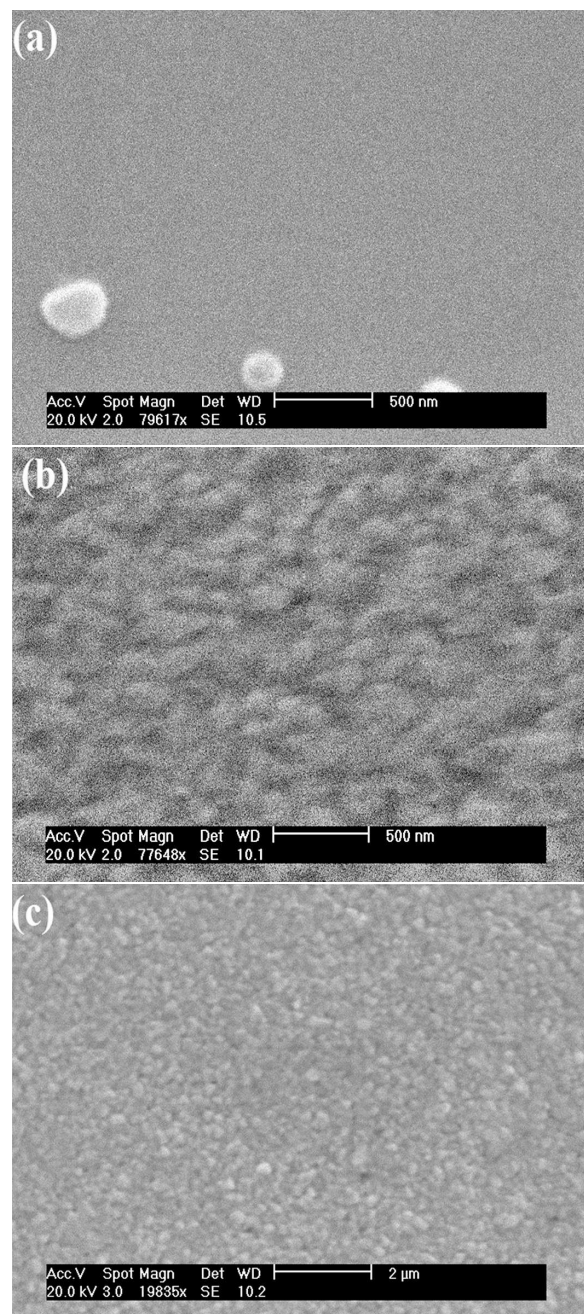


Fig. 3. SEM images of (a) CdS thin films and PbS films (b) with and (c) without TEA.

a continuous and compact polycrystalline films with well-defined grain boundaries. The grain sizes were estimated from SEM images to be 26 nm, 270 nm and 15 nm for PbS-A, PbS-B and CdS films, respectively. The crystallite sizes in the SEM images are greater than that obtained from the XRD

patterns. Larger clusters, deposited on the surface of the film, clearly show an aggregate structure composed of small crystals or grains and SEM images show these clusters on the surface of the film. But in XRD method, the patterns were reflected from small crystals or grains.

### 3.3. Optical properties

Fig. 4 shows the optical absorption of CdS sample at the wavelengths range of 300 nm to 1100 nm which shows a low absorption in visible region, thus making CdS a good candidate for a transparent window in solar cells. The inset in Fig. 4 presents the diagram normally used to determine the band-gap of films. The obtained band gap for CdS film is about 2.68 eV, which is higher than the CdS bulk band-gap value, due to quantum confinement effect in the nanocrystalline CdS films. The increased effective band gap causes nanocrystalline CdS films to be a more suitable window material in solar cell applications.

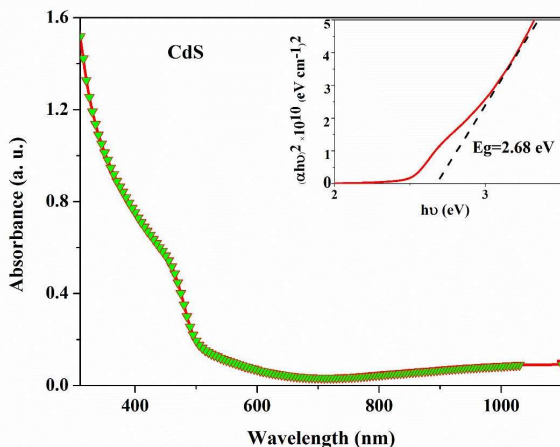


Fig. 4. The optical absorption of CdS sample at wavelengths of 300 nm to 1100 nm. The inset presents the diagram normally used to determine the band-gap of films.

Fig. 5 shows the transmittance and reflectance of CdS thin film from the near-ultraviolet (300 nm) to the near-infrared (1100 nm) region. The CdS film exhibits high transmittance and low reflectance in the visible region. The sharp increase of transmission starts at around 460 nm, in agreement with the band gap of approximately 2.6 eV; the average

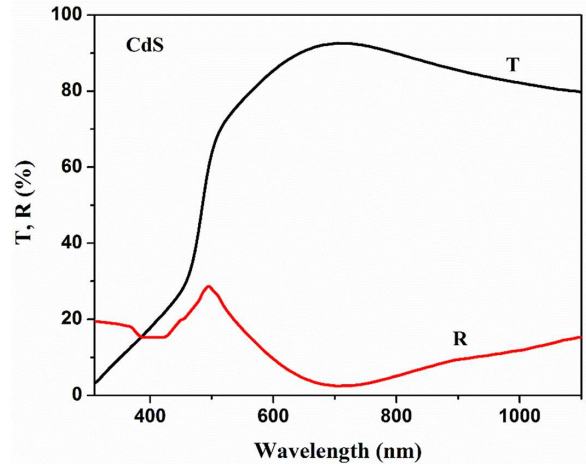


Fig. 5. The transmittance and reflectance of CdS thin film from the near-ultraviolet (300 nm) to the near-infrared (1100 nm) regions.

reflectance of 14 % is related to the transmission losses in the transparency region and is the result of comparatively high refractive index  $n$  (around 2.3) of the material. The reflection minimum at 700 nm and corresponding maximum in transmission (90 %) are observed.

The transmission and reflection spectra of PbS films with different thicknesses (200 nm for PbS-A and 800 nm for PbS-B), deposited on glass, in the spectral range of 300 nm to 2600 nm, are shown in Fig. 6. In all cases, a clear interference pattern is seen. It shows that for the PbS-A and PbS-B films, the transmittance began to increase at 700 nm and 1200 nm, respectively (Fig. 6a). A decrease in transmission with increasing thickness of the films is also observed. The PbS-B film has lower transmission and reflection value than PbS-A in the visible range. These results indicate that the PbS-B film is a good absorber layer so, it can be considered as a potential material for solar cell applications due to the low transmittance in visible range. The determined energy gap for PbS thin films was found to be 1.47 eV and 0.64 for PbS-A and PbS-B, respectively (Fig. 7).

### 3.4. Solar cell characteristics

Fig. 8 shows the (J-V) characteristics of typical solar cells fabricated using CBD under

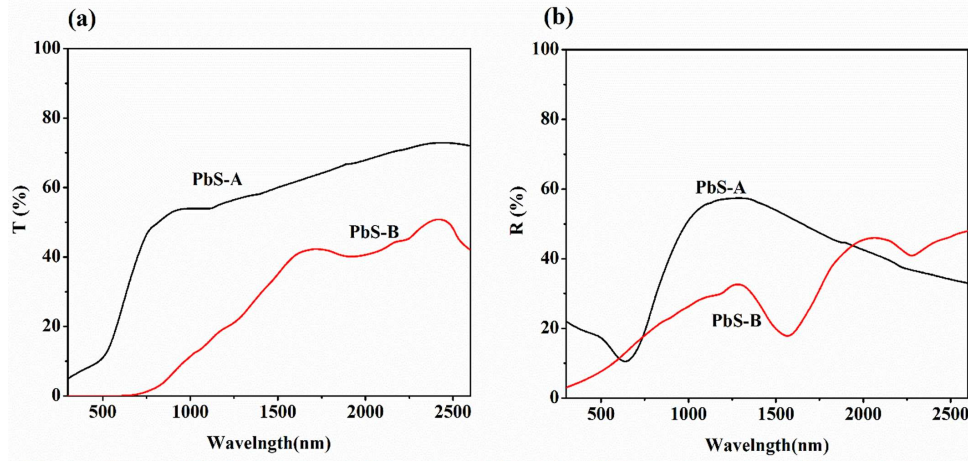


Fig. 6. The transmission and reflection spectra of PbS films with different thicknesses, 200 nm for PbS-A and 800 nm for PbS-B, deposited on glass in the spectral range of 300 nm to 2600 nm.

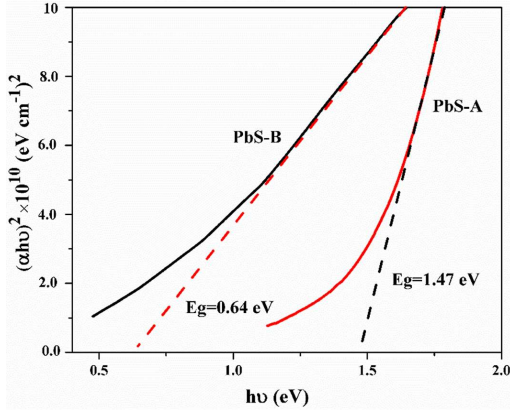


Fig. 7. Variation of  $(\alpha h\nu)^2$  with photon energy for PbS thin films. The estimated band gap is about 1.47 eV for PbS-A and 0.64 eV for PbS-B.

illumination condition of  $90 \text{ mW/cm}^2$ . Two types of solar cells for different PbS absorber layers (prepared with and without TEA) have been analyzed. The one with 1 M TEA concentration is denoted as solar cell with PbS-A absorbing layer (SC/PbS-A) and the other without TEA is denoted as solar cell with PbS-B absorbing layer (SC/PbS-B). The solar cells structures have an open-circuit voltage ( $V_{oc}$ ) of 285 mV for SC/PbS-A and 275 mV for SC/PbS-B and a short-circuit current density ( $J_{sc}$ ) of  $9.41 \text{ mA/cm}^2$  for SC/PbS-A and  $12.24 \text{ mA/cm}^2$  for SC/PbS-B. The results reveal that without TEA, the open-circuit voltage

decreases which may be due to the decreased energy band gap. The maximum voltage ( $V_{max}$ ) and maximum current ( $J_{max}$ ) are  $V_{max} = 150 \text{ mV}$  and  $J_{max} = 7.74 \text{ mA/cm}^2$  for SC/PbS-A and  $V_{max} = 165 \text{ mV}$  and  $J_{max} = 7.11 \text{ mA/cm}^2$  for SC/PbS-B. Resistive effects in solar cells reduce the efficiency of the solar cell by dissipating power in the resistances [17]. In the high field regime, the series resistance ( $R_s$ ) dominates and can be determined from the relationship as [18]:

$$\frac{dI}{dV_{I=0}} = \frac{1}{R_s} \quad (2)$$

In the low field regime, the shunt resistance ( $R_{sh}$ ) dominates and can be determined as [18]:

$$\frac{dI}{dV_{V=0}} = \frac{1}{R_{sh}} \quad (3)$$

The (J-V) characteristics depend on the series and shunt resistances. Ideal solar cells have a zero series resistance and infinite shunt resistance. From equation 2 and equation 3, we obtained  $R_s = 140 \Omega$ , for SC/PbS-A and  $R_s = 500 \Omega$  for SC/PbS-B. We see that by adding TEA, the resistance decreases. The shunt resistance is  $R_{sh} = 249 \Omega$  for SC/PbS-A and  $R_{sh} = 5500 \Omega$  for SC/PbS-B.

The fill factor (FF) was calculated from the following relationship [19]:

$$FF = \frac{J_M \times V_M}{J_{sc} \times V_{oc}} \quad (4)$$

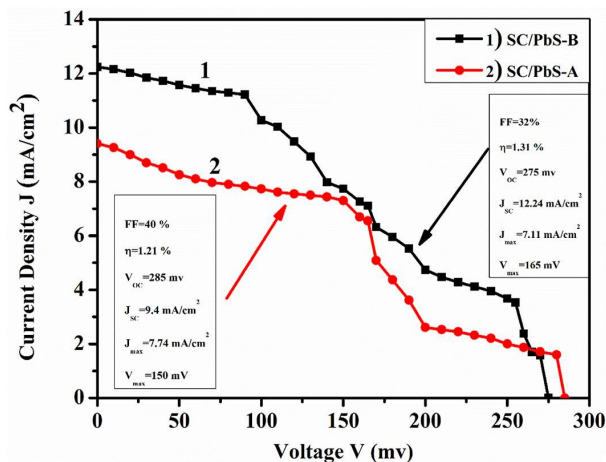


Fig. 8. The (J-V) characteristics of SCPbS-A and SCPbS-B solar cells under illumination condition of  $90 \text{ mW/cm}^2$ .

The FF is 40 % for SC/PbS-A and 32 % for SC/PbS-B. This lower value of the FF may be a sign of slightly more efficient recombination of the electron hole pairs in the active layer.

The energy conversion efficiency  $\eta$  can be calculated using the equation [19]:

$$\eta = FF \frac{J_{sc} \times V_{oc}}{P_{in}} \quad (5)$$

The efficiency of the solar cells was found to be 1.21 % for SC/PbS-A and 1.31 % for SC/PbS-B, showing that adding TEA decreases the efficiency of the cells. It is believed that when we add TEA, the energy gap increases, leading to a decrease in electron hole pairs.

## 4. Conclusions

A simple and efficient technique was used to fabricate ITO/CdS/PbS solar cell using CBD method. The synthesized thin films of good quality were fabricated and their morphology studied by SEM revealed a uniform surface over the entire substrate. XRD analysis revealed that the prepared thin films have good crystalline quality. XRD and SEM observations revealed that the thin films were influenced by adding TEA. We showed that adding TEA to the solution decreases the series resistance, increases the shunt resistance and

decreases the grain size, which results in a decrease in the efficiency of the fabricated solar cell. This issue is attributed to the crystallite size in the prepared thin films.

Future works would be directed towards understanding the treatment conditions that can enhance the efficiency of the solar cells.

## References

- [1] EMIN S., SINGH S.P., HAN L., SATOH N., ISLAM A., *Sol. Energy*, 85 (2011), 1264.
- [2] ZHANG J.Z., *Optical Properties and Spectroscopy of Nanomaterials*, World Scientific Publishing, London, 2009, p.136.
- [3] GUNES S., FRITZ K.P., NEUGEBAUER H., SARICTICI N.S., KUMAR S., SCHOLES G.D., *Sol. Energ. Mat. Sol. C.*, 91 (2007), 420.
- [4] DHANAM M., KAVITHA B., MAHESWARI B., JESNA G.R., *Acta Phys. Pol. A*, 119 (2011), 885.
- [5] NAIR P.K., NAIR M.T.S., GARCIA V.M., ARENAS O.L., PEÑA Y., CASTILLO A., AYALA I.T., GOMEZDAZA O., SÁNCHEZ A., CAMPOS J., HU H., SUÁREZ R., RINCÓN M.E., *Sol. Energ. Mat. Sol. C.*, 52 (3 – 4) (1998), 313.
- [6] TOHIDI T., JAMSHIDI-GHALEH K., NAMDAR A., ABDI-GHALEH R., *Mat. Sci. Semicon. Proc.*, 25 (2014), 197.
- [7] PAWAR S.M., PAWAR B.S., KIM J.H., JOO O.-S., LOKHANDE C.D., *Curr. Appl. Phys.*, 11 (2011), 117.
- [8] HODES G., *Phys. Chem. Chem. Phys.*, 9 (2007), 2181.
- [9] DOBSON K.D., VISOLY-FISHER I., HODES G., CAHEN D., *Sol. Energ. Mat. Sol. C.*, 62 (2000), 295.
- [10] SCHEER R., SCHOCK H.W., *Chalcogenide Photo-voltaics: Physics, Technologies and Thin Film Devices*, John Wiley & Sons, 2011.
- [11] NAIR P.K., BARRIOS-SALGADO E., CAPISTRÁN J., RAMÓN M.L., NAIR M.T.S., ZINGARO R.A., *J. Electrochem. Sci. Te.*, 157 (2010), D528.
- [12] BHANDARI K.P., ROLAND P.J., MAHABADUGE H., HAUGEN N.O., GRICE C.R., JEONG S., DYKSTRA T., GAO J., ELLINGSON R.J., *Sol. Energ. Mat. Sol. C.*, 117 (2013), 476.
- [13] HERNANDEZ-BORJA J., VOROBIEVN Y.V., RAMIREZ-BON R., *Sol. Energ. Mat. Sol. C.*, 95 (2011), 1882.
- [14] OBAID A.S., HASSAN Z., MAHDI M.A., BOUOUDINA M., *Sol. Energy*, 89 (2013), 143.
- [15] TOHIDI T., JAMSHIDI-GHALEH K., *Appl. Phys. A*, 118 (2015), 1247.
- [16] JUNG S., AHN S., YUN J.H., GWAK J., KIMB D., YOON K., *Curr. Appl. Phys.*, 10 (2010), 990.
- [17] LEE M.-K., WANG J.-C., HORNG S.-F., MENG H.-F., *Sol. Energ. Mat. Sol. C.*, 94 (2010), 578.
- [18] BAROTE M.A., YADAV A.A., CHAVANAN T.V., MASUMDAR E.U., *Dig. J. Nanomater. Bios.* 6 (2011), 979.

- [19] WANG Z.S.Q., ZENG X., ZHANG C., SHI M., TAN F.,  
WANG Z., LIUB J., HOUC Y., TENG C F., FENG C Z.,  
*Polymer*, 49 (2008), 4647.

*Received 2015-10-08*  
*Accepted 2016-05-30*